Elastic and piezoelectric fields around a quantum dot: Fully coupled or semicoupled model?

E. Pan[a)]
Structures Technology Incorporated, 543 Keisler Drive, Suite 204, Cary, North Carolina 27511

(Received 1 October 2001; accepted for publication 18 December 2001)

In the study of elastic and piezoelectric fields in semiconductors due to buried quantum dots (QDs), the semicoupled piezoelectric model is commonly adopted. However, its accuracy and suitability have never been studied. In this article, by developing a fully coupled piezoelectric model and deriving the analytical elastic and piezoelectric fields based on this and the semicoupled models, we are able to verify that when the piezoelectric coupling is weak, like GaAs with the electromechanical coupling factor $g=0.04$, the semicoupled model predicts very accurate results as compared to those based on the fully coupled model. However, if the piezoelectric coupling is relatively strong, like AlN with $g=0.32$, we have shown that the semicoupled model gives very serious errors or even totally wrong results. Applying these two models to a uniformly strained AlN layer grown along the polar axis has also confirmed our observation. Therefore, for semiconductors like AlN, the fully coupled model presented in this article must be employed in order to give a reliable and accurate prediction for the elastic and piezoelectric fields. Also presented in this article is the distribution of the piezoelectric field on the surface of a half-space GaAs due to a buried QD located at 2 nm below the surface with a volume $4\pi/3$ $(\text{nm})^3$. It is observed that the horizontal electric field on the traction-free and insulating surface shows some special features and its maximum magnitude can be as high as 3.5×10^7 V/m when the uniform mismatch eigenstrain is 0.07. Furthermore, the piezoelectric field on the traction-free and conducting surface exhibits different characters as compared to the traction-free and insulating case. © *2002 American Institute of Physics.* [DOI: 10.1063/1.1448869]

I. INTRODUCTION

A buried quantum dot (QD), i.e., an eigenstrain due to the lattice mismatch between the QD and the surrounding piezoelectric matrix, induces not only an elastic field, but also a piezoelectric field. Since both the elastic and piezoelectric fields are equally important in the understanding of the photonic and electronic features in semiconductors,[1–3] a reliable analysis on these fields are crucial to the design of such structures. It is obvious that a decoupled model without consideration of the effect of the elastic field on the piezoelectric field, or vice versa, is unsuitable. Therefore, a fully coupled or at least a semicoupled model should be used, with the later being commonly adopted in physical community for the prediction of the piezoelectric field. In such a simplified model, the QD-induced elastic field is first solved, either analytically (when the geometry is simple and/or the involved elastic material is isotropic)[4] or numerically otherwise using either the finite element method or the finite difference method.[5–8] The purely elastic solution (actually the elastic strain or stress tensor) is then used to find the polarization field, which induces the electric potential and electric field. Finally, the induced piezoelectric field is solved under suitable purely piezoelectric boundary conditions. This semicoupled model was previously applied to various semiconductors, such as group III–V[4,8] and group III nitrides.[9] So far, however, no fully coupled piezoelectric model has ever been proposed and applied to the study of the QD-induced elastic and piezoelectric fields. Furthermore, whether the semicoupled model is suitable or not, a key and fundamental question, has never been answered in the literature.

In a recent article, the author[10] solved the generalized Mindlin's problem in a fully coupled and generally anisotropic piezoelectric half space where the point source can be either the elastic point-force or the electric point-charge density. By examining two typical piezoelectric materials, one is strongly coupled and the other is weakly coupled, the author has been able to demonstrate the importance and necessity of using the fully coupled piezoelectric model in the prediction of the elastic and piezoelectric fields induced by a point force/point charge. We further remark that Ru[11,12] solved the corresponding half-plane problem and his solution for an inclusion of any shape has also shown analytically the effect of the electromechanical coupling on the elastic and piezoelectric fields.

In this article, we introduce a fully coupled piezoelectric model for the prediction of the QD-induced elastic and piezoelectric fields in semiconductors by employing the generalized Betti's reciprocal theorem and the point-force/point-charge solutions recently developed by the author.[10] Furthermore, a detailed study on the semicoupled model is also given. Assuming elastic isotropy (only for the purpose of simplifying the derivation of the solution for the semicoupled model) for the semiconductors GaAs and AlN, we have derived the analytical solutions, based on the semicoupled model, for the elastic and piezoelectric fields in a

a)Electronic mail: ernian_pan@yahoo.com

full- and half-space GaAs, and in a full-space AlN. Therefore, with these solutions, a quantitative assessment on the suitability of the semicoupled model is carried out (as compared to the results based on the fully coupled model). It is found that the semicoupled model can predict very accurately the elastic and piezoelectric fields induced by a QD in the full- and half-space GaAs. However, the semicoupled model gives serious errors or completely wrong results for the elastic and piezoelectric fields in AlN. This important observation has been further confirmed by applying the fully coupled and semicoupled models to a uniformly strained AlN layer grown along the polar axis.

Finally, this article presents the distribution of the piezoelectric field on the surface of a half-space GaAs due to a buried QD located at 2 nm below the surface with a volume $4\pi/3\ (\text{nm})^3$. It is observed that the horizontal electric field on the traction-free and insulating surface possesses some special features and its maximum magnitude can be as high as 3.5×10 V/m when the uniform mismatch eigenstrain is 0.07. Furthermore, the piezoelectric field on the traction-free and conducting surface exhibits completely new characters as compared to the traction-free and insulating case. All results presented can be served as benchmark examples for future researchers in this area and should be also of great interest to the QD device analysis.

II. FULLY COUPLED MODEL

We consider the fully coupled deformation of a linearly anisotropic piezoelectric semiconductor due to a point force/point charge applied at the source point **y** within the given semiconductor. The equilibrium equations can be expressed as[10,13–15]

$$\sigma_{ji,j}+f_i\delta(\mathbf{x}-\mathbf{y})=0;\quad D_{i,i}-q\,\delta(\mathbf{x}-\mathbf{y})=0, \tag{1}$$

where σ_{ij} and D_i are, respectively, the elastic stress and electric displacement; and f_i and q are, respectively, the amplitudes of the point force and point charge. As a convention, lowercase (uppercase) subscripts always range from 1 to 3 (1 to 4) and summation over repeated lowercase (uppercase) subscripts is implied. A subscript comma denotes the partial differentiation with respect to the coordinates.

For a fully coupled piezoelectric solid, the elastic deformation and electric field are coupled together by the following constitutive relations[14,16]

$$\begin{aligned}\sigma_{ij}&=C_{ijlm}\gamma_{lm}-e_{kji}E_k,\\ D_i&=e_{ijk}\gamma_{jk}+\epsilon_{ij}E_j,\end{aligned} \tag{2a,b}$$

where C_{ijlm}, e_{ijk}, and ϵ_{ij} are, respectively, the elastic moduli, piezoelectric coefficients, and dielectric constants. The elastic strain γ_{ij} and electric field E_i in (2a,b) are related to the elastic displacement u_i and electric potential ϕ, respectively, by

$$\gamma_{ij}=\frac{1}{2}(u_{i,j}+u_{j,i});\quad E_i=-\phi_{,i}. \tag{3a,b}$$

We point out that the decoupled state (purely elastic and purely electric deformations) can be obtained by simply setting $e_{ijk}=0$ in (2a,b), one of the procedures adopted in almost all previous studies in strained quantum devices. Another one is to use the semicoupled model where constitutive relation (2a) is used to find the purely elastic field by dropping the second term on the right-hand side (i.e., $e_{ijk}=0$), and relation (2b) is then used to estimate the electric field induced by the purely elastic field (i.e., the elastic strain tensor with $e_{ijk}\neq 0$). It is obvious that if one is also interested in the piezoelectric field, the fully coupled or at least the semicoupled model should be used.

The fully coupled elastic and piezoelectric fields can be conveniently studied using the Barnett–Lothe notation.[15] In terms of this notation, the elastic displacement u_i and electric potential ϕ, the elastic strain γ_{ij} and electric field E_i, the elastic stress σ_{ij} and electric displacement D_i, and the elastic and electric moduli (C_{ijlm}, e_{ijk}, and ϵ_{ij}) can be grouped together as:[10,13,15,17]

$$u_I=\begin{cases}u_i, & I=1,2,3\\ \phi, & I=4\end{cases}, \tag{4}$$

$$\gamma_{Ij}=\begin{cases}\gamma_{ij}, & I=1,2,3\\ -E_j, & I=4\end{cases}, \tag{5}$$

$$\sigma_{iJ}=\begin{cases}\sigma_{ij}, & J=1,2,3\\ D_i, & J=4\end{cases}, \tag{6}$$

$$C_{iJKl}=\begin{cases}C_{ijkl}, & J,K=1,2,3\\ e_{lij}, & J=1,2,3;\quad K=4\\ e_{ikl}, & J=4;\quad K=1,2,3\\ -\epsilon_{il}, & J=K=4\end{cases}. \tag{7}$$

In terms of this shorthand notation, the constitutive relations (2a,b) can be unified into

$$\sigma_{iJ}=C_{iJKl}\gamma_{Kl}. \tag{8}$$

Similarly, the equilibrium Eq. (1) in terms of the elastic stress/electric displacement can be recast into

$$\sigma_{iJ,i}+f_J=0, \tag{9}$$

with f_J being defined as

$$f_J=\begin{cases}f_j\delta(\mathbf{x}-\mathbf{y}), & J=1,2,3\\ -q\,\delta(\mathbf{x}-\mathbf{y}), & J=4\end{cases}. \tag{10}$$

The fully coupled piezoelectric model is now applied to the calculation of the elastic and piezoelectric fields in a full- and half-spaces due to a buried QD. These induced fields are expressed in terms of boundary integrals on the surface of the QD for a finite-size QD, and in terms of the point-force/point-charge Green's function solutions for a point QD. The generalized Betti's reciprocal theorem is employed to derive these elastic and piezoelectric fields.

A general eigenstrain problem in an anisotropic and linearly piezoelectric semiconductor (full or half space) can be reduced to an integral equation in terms of the associated point-force/point-charge Green's functions. This integral expression is a consequence of the Betti's reciprocal theorem in piezoelectricity.[13] We assume that there are two states associated with the problem domain: One is the eigenstrain problem, i.e., an eigenstrain γ^*_{Ij} (elastic strain and electric field,

with $I=4$ for the latter) in a finite subdomain Ω of the full- or half-space D, and the other is the point-force/point-charge Green's function problem. Then the elastic displacement and electric potential $u_K(\mathbf{y})$ due to the eigenstrain γ_{Ij} can be expressed by

$$u_K(\mathbf{y})=\int_{\partial D}[u_J^K(\mathbf{x};\mathbf{y})\sigma_{iJ}(\mathbf{x})n_i(\mathbf{x}) - \sigma_{iJ}^K(\mathbf{x};\mathbf{y})n_i(\mathbf{x})u_J(\mathbf{x})]dS(\mathbf{x}) + \int_D u_J^K(\mathbf{x};\mathbf{y})[-C_{iJLm}\gamma_{Lm}^*(\mathbf{x})]_{,i}]dV(\mathbf{x}), \quad (11)$$

where ∂D is the boundary of D which is a spherical surface with a large radius for the full-space case, and the surface of the half-space and a half spherical surface with a large radius for the half-space case; $u_J^K(\mathbf{x},\mathbf{y})$ and $\sigma_{iJ}^K(\mathbf{x};\mathbf{y})$ are the Green's J-th elastic displacement/electric potential and iJ-th stress components/electric displacements at $\mathbf{x}$ due to a point force/point charge in the K-th direction applied at $\mathbf{y}$. While Pan and Tonon[18] obtained the full-space Green's functions, Pan and Yuan[19] derived those in a half space under the traction-free and insulating surface condition. More recently, Pan[10] solved the generalized Mindlin problem where the surface of the piezoelectric half-space is under general boundary conditions. These Green's functions, along with their derivatives with respect to the source coordinate $\mathbf{y}$, are summarized in Appendices A and B for the sake of easy reference.

Notice that since the eigenstrain γ_{Ij}^* is applied only in the finite subdomain Ω of D and that the boundary ∂D is either in infinity where the integrands are zero or the surface of the half space on which the Green's functions are zero, it is evident that the integration on the boundary ∂D in Eq. (11) is zero. Therefore, Eq. (11) is reduced to

$$u_K(\mathbf{y})=\int_D u_J^K(\mathbf{x};\mathbf{y})[-[C_{iJLm}\gamma_{Lm}^*(\mathbf{x})]_{,i}]dV(\mathbf{x}). \quad (12)$$

Differentiation in Eq. (12) can be shifted by applying the Gauss theorem and by noticing that the eigenstrain is nonzero only in Ω, which gives

$$u_K(\mathbf{y})=\int_\Omega C_{iJLm}u_{J,x_i}^K(\mathbf{x};\mathbf{y})\gamma_{Lm}^*(\mathbf{x})dV(\mathbf{x}). \quad (13)$$

The domain integral in Eq. (13) can be further transformed to the surface of Ω if the eigenstrain is constant. That is

$$u_K(\mathbf{y})=C_{iJLm}\gamma_{Lm}^*\int_{\partial\Omega}u_J^K(\mathbf{x};\mathbf{y})n_i(\mathbf{x})dS(\mathbf{x}), \quad (14)$$

where $n_i(\mathbf{x})$ are the outward normal components on the surface of Ω.

To find the elastic strain and electric fields, we take the derivatives of Eq. (14) with respect to the observation point $\mathbf{y}$ (i.e., the source point of the point-force/point-charge Green's function), which yields

$$\gamma_{kp}(\mathbf{y})=\frac{1}{2}\gamma_{Lm}^*\int_{\partial\Omega}C_{iJLm}[u_{J,y_p}^k(\mathbf{x};\mathbf{y}) + u_{J,y_k}^p(\mathbf{x};\mathbf{y})]n_j(\mathbf{x})dS(\mathbf{x}); \quad k=1,2,3, \quad (15a)$$

$$\gamma_{Kp}(\mathbf{y})=\gamma_{Lm}^*\int_{\partial\Omega}C_{iJLm}u_{J,y_p}^K(\mathbf{x};\mathbf{y})n_j(\mathbf{x})dS(\mathbf{x}); \quad K=4 \quad (15b)$$

with the corresponding stress and electric displacement fields being

$$\sigma_{iJ}(\mathbf{y})=C_{iJKp}[\gamma_{Kp}(\mathbf{y})-\chi\gamma_{Kp}^*] \quad (16)$$

where χ equals to 1 if the observation point $\mathbf{y}$ is within the eigenstrain domain Ω, and 0 otherwise.

Finally, for a point (or concentrated) eigenstrain applied at point $\mathbf{x}$, the induced elastic displacement/electric potential and elastic strain/electric fields can be expressed directly by the point-force/point-charge Green's functions without either volumetric or surface integration. Assuming that the point eigenstrain or point QD has an equal intensity of a sphere with radius a (i.e., with a volume $v_a=4\pi a^3/3$) centered at $\mathbf{x}$, then the QD-induced elastic displacement/electric potential and strain/electric fields are found to be, respectively,

$$u_K(\mathbf{y})=\sigma_{mL}^K(\mathbf{x};\mathbf{y})\gamma_{Lm}^*v_a \quad (17)$$

and

$$\gamma_{kp}(\mathbf{y})=\frac{1}{2}\gamma_{Lm}^*[\sigma_{mL,p_y}^k(\mathbf{x};\mathbf{y})+\sigma_{mL,k_y}^p(\mathbf{x};\mathbf{y})]v_a; \quad k=1,2,3 \quad (18a)$$

$$\gamma_{Kp}(\mathbf{y})=\gamma_{Lm}^*\sigma_{mL,p_y}^K(\mathbf{x};\mathbf{y})v_a; \quad K=4 \quad (18b)$$

Equation (17) indicates that the elastic displacement/electric potential at $\mathbf{y}$ in the K-th direction ($K=4$ for the electric potential) due to a QD at $\mathbf{x}$ with components (Lm) ($L=4$ for the electric field) is equivalent to the elastic stress/electric displacement field at $\mathbf{x}$ with components (mL) ($L=4$ for the electric displacement) due to a point force/point charge at $\mathbf{y}$ in the K-th direction ($K=4$ for the point-charge). We remark that while a similar observation can be made for Eq. (18), this equivalent property, between a point force/point charge and a point eigenstrain (or point QD), is an extension to the piezoelectricity of the purely elastic equivalent property between a point-force and a point-dislocation solution.[20,21]

III. SEMICOUPLED MODEL

In the semicoupled model, the purely elastic problem [i.e., using Eq. (2a) with $e_{ijk}=0$] due to a QD is solved first, subject to the given elastic boundary condition if any boundary exists.

After the elastic strain tensor γ_{ij} is obtained, the following relation is then used to find the QD-induced polarization field P_i,[1,4]

$$P_i=e_{ijk}\gamma_{jk}. \quad (19)$$

It is seen that this relation is actually quite similar to Eq. (2b) with ϵ_{ij} being zero. The electric field is solved using the following governing equations subject to the electric boundary condition if any boundary exists:[1,16]

$$D_{i,i}=\rho_e; \quad \eta_{ijk}E_{j,k}=0; \quad D_i=\epsilon_{ij}E_j+P_i, \qquad (20a,b,c)$$

where ρ_e is the external charge density; η_{ijk} the alternating symbol which equals 1 if (ijk) is a cyclic permutation of (123), equals -1 if (ijk) is an anticyclic permutation of (123), and equals 0 otherwise. It is obvious that Eq. (20b) for the electric field E_i is automatically satisfied if Eq. (3b) is used. Expressing the electric field by the gradient of the electric potential in Eq. (20c) and substituting the result into Eq. (20a) gives the following equation for the electric potential

$$\epsilon_{ij}\phi_{,ij}=-\rho_e+P_{k,k}. \qquad (21)$$

Thus, $P_{k,k}$ can be seen alternatively as a negative charge density.[4,8]

Since the equivalent charge density $P_{k,k}$ is related to the purely elastic strain field, an exact closed-form solution to Eq. (21) exists only for certain elastic materials in either full- or half-space.[22–26] Therefore, to simplify our derivation and arrive at some analytical results using the semicoupled model for the purpose of comparison with the fully coupled model, we assume that the elastic moduli of the semiconductor material is isotropic.

IV. SEMICOUPLED SOLUTION IN A FULL SPACE

We now apply the semicoupled model to find the elastic and piezoelectric fields in a semiconductor full space due to a buried QD. Both the GaAs and AlN semiconductors will be considered. While GaAs is a weakly coupled material with an electromechanical coupling factor $g=0.04$, AlN is a strongly coupled one with $g=0.32$. It is also noticed that in order to find the piezoelectric field, one has to derive first the corresponding purely elastic solution due to the QD. This is presented next.

A. Purely elastic solution in a full space

Assuming that the purely elastic full space is isotropic, and that a uniform QD with a hydrostatic strain $\gamma_{ij}^*=\gamma^0\delta_{ij}$ and an intensity equal to that of a sphere with a radius a (i.e., $v_a=4\pi a^3/3$) is located at $\mathbf{x}=(0,0,0)$, then the only nonzero elastic displacement induced by this QD is in the radial direction of the spherical coordinates.[4,23,27] That is

$$u_r(r)=\frac{\gamma^0 v_a(1+\nu)}{4\pi(1-\nu)r^2}. \qquad (22)$$

Introducing an elastic displacement potential function as

$$u_i=\psi_{,i}; \quad i=1,2,3, \qquad (23)$$

$$\psi=-\frac{\gamma^0 v_a(1+\nu)}{4\pi(1-\nu)r}, \qquad (24)$$

the elastic strain and stress tensors are readily to be obtained as

$$\gamma_{ij}=\psi_{,ij}; \quad i,j=1,2,3$$
$$\sigma_{ij}=C_{ijkl}\psi_{,kl}, \qquad (25a,b)$$

where C_{ijkl} is the fourth-order stiffness tensor, which is characterized by two elastic constants for the isotropic case.

B. Piezoelectric fields in full-space GaAs

Since the only nonzero piezoelectric constant in GaAs is e_{14} ($=e_{25}=e_{36}$), the polarization field based on Eq. (19) of the semi-coupled model is therefore reduced to

$$P_x=2e_{14}\gamma_{yz}; \quad P_y=2e_{14}\gamma_{zx}; \quad P_z=2e_{14}\gamma_{xy}. \qquad (26)$$

Using Eq. (23)–(25), the polarization field can be easily found as

$$P_x=2e_{14}\psi_{,yz}=-\frac{3e_{14}\gamma^0 v_a(1+\nu)}{2\pi(1-\nu)}\frac{yz}{r^5},$$
$$P_y=2e_{14}\psi_{,xz}=-\frac{3e_{14}\gamma^0 v_a(1+\nu)}{2\pi(1-\nu)}\frac{xz}{r^5}, \qquad (27)$$
$$P_z=2e_{14}\psi_{,xy}=-\frac{3e_{14}\gamma^0 v_a(1+\nu)}{2\pi(1-\nu)}\frac{xy}{r^5},$$

which yields

$$P_{k,k}=6e_{14}\psi_{,xyz}. \qquad (28)$$

Thus, the electric potential should satisfy the following Poisson's equation

$$\phi_{,kk}=\frac{6e_{14}}{\epsilon_0\epsilon_r}\psi_{,xyz}, \qquad (29)$$

which permits a solution as[4]

$$\phi=-\frac{9\gamma^0 v_a(1+\nu)e_{14}}{4\pi(1-\nu)\epsilon_0\epsilon_r}\frac{xyz}{r^5}. \qquad (30)$$

While the electric field E_i can be obtained by taking the derivative of the electric potential, the electric displacement D_i can be found using Eq. (20c) along with the polarization field (27).

C. Piezoelectric fields in full-space AlN

For a wurtzite AlN, the polarization field is related to the strain tensor as[9,16]

$$\begin{bmatrix} P_x \\ P_y \\ P_z \end{bmatrix}=\begin{bmatrix} 0 & 0 & 0 & 0 & e_{15} & 0 \\ 0 & 0 & 0 & e_{15} & 0 & 0 \\ e_{31} & e_{31} & e_{33} & 0 & 0 & 0 \end{bmatrix}\begin{bmatrix} \gamma_{xx} \\ \gamma_{yy} \\ \gamma_{zz} \\ 2\gamma_{yz} \\ 2\gamma_{zx} \\ 2\gamma_{xy} \end{bmatrix}. \qquad (31)$$

We mention that this structure is also called transversely isotropic with the poling direction along the z axis.

Similarly, using the solved elastic strain field (25a), the polarization field is found to be

$$P_x=2e_{15}\psi_{,xz}=-\frac{3e_{15}\gamma^0 v_a(1+\nu)}{2\pi(1-\nu)}\frac{xz}{r^5},$$

$$P_y=2e_{15}\psi_{,yz}=-\frac{3e_{15}\gamma^0 v_a(1+\nu)}{2\pi(1-\nu)}\frac{yz}{r^5}, \tag{32}$$

$$P_z=e_{31}(\psi_{,xx}+\psi_{,yy})+e_{33}\psi_{,zz}$$
$$=\frac{\gamma^0 v_a(1+\nu)}{4\pi(1-\nu)}(e_{31}-e_{33})\left[\frac{2}{r^3}-\frac{3(x^2+y^2)}{r^5}\right],$$

which gives

$$P_{k,k}=(2e_{15}+e_{31})(\psi_{,xxz}+\psi_{,yyz})+e_{33}\psi_{,zzz}. \tag{33}$$

Consequently, the electric potential satisfies the following Poisson's equation

$$\phi_{,kk}=\frac{1}{\epsilon_0\epsilon_r}[(2e_{15}+e_{31})(\psi_{,xxz}+\psi_{,yyz})+e_{33}\psi_{,zzz}] \tag{34}$$

from which, a solution is found as

$$\phi=-\frac{3\gamma^0 v_a(1+\nu)(2e_{15}+e_{31}-e_{33})z}{8\pi(1-\nu)\epsilon_0\epsilon_r}$$
$$\times\left\{\frac{(x^2+y^2)}{r^5}-\frac{2}{5r^3}\right\}. \tag{35}$$

Again, similar to the GaAs case, the electric field is obtained by taking the derivative of the electric potential, and the electric displacement field is then obtained using Eq. (20c) with the given polarization field (32).

We will numerically show later that in the full-space GaAs where the electromechanical coupling is weak, the semicoupled model predicts nearly identical elastic and electric fields as those based on the fully coupled rigorous model. However, the semicoupled model gives completely wrong results for both the elastic and electric fields in the full-space AlN where the electromechanical coupling is strong. It is therefore concluded that even for the full-space AlN, the semicoupled model should not be used! While the semicoupled model can be safely used for the full-space GaAs to study the QD-induced elastic and piezoelectric fields, its suitability and accuracy to the half-space GaAs is explored in the next section.

V. HALF-SPACE GaAs

When a QD is located close to the surface, the influence of the surface must be considered. In this situation, the analytical solution developed in the previous section for a QD in a full-space can not be used. Instead, the solution in a half-space based on the semicoupled model needs to be derived. Following the similar procedure, we first derive the elastic field and then the piezoelectric field.

A. Purely elastic solution in half-space GaAs

Let us again assume that a QD with a uniform hydrostatic strain $\gamma_{Ij}^*=\gamma^0\delta_{ij}$ and a volume $v_a=4\pi a^3/3$ is centered at a distance $z=h$ below the surface of the half-space GaAs (Fig. 1). We further define

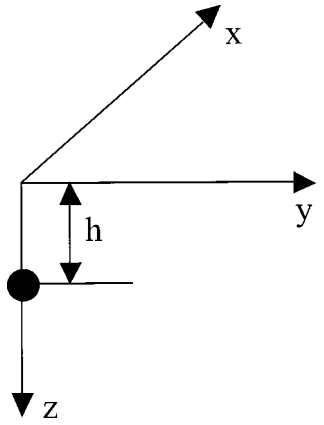

FIG. 1. QD at $z=h$ (nm) below the surface of a half space.

$$R_1=\sqrt{x^2+y^2+(z-h)^2}$$
$$R_2=\sqrt{x^2+y^2+(z+h)^2}. \tag{36}$$

Then, the elastic displacements in the half space due to the QD can be found as[22,23,27]

$$u_x=\frac{\gamma^0 v_a(1+\nu)x}{4\pi(1-\nu)}\left\{\frac{1}{R_1^3}+\frac{3-4\nu}{R_2^3}-\frac{6z(z+h)}{R_2^5}\right\}. \tag{37}$$

While u_y can be obtained from Eq. (37) by replacing the variable x with y, u_z is expressed as

$$u_z=\frac{\gamma^0 v_a(1+\nu)}{4\pi(1-\nu)}\left\{\frac{z-h}{R_1^3}-\frac{(3-4\nu)(z+h)}{R_2^3}+\frac{2z}{R_2^3}\right.$$
$$\left.-\frac{6z(z+h)^2}{R_2^5}\right\}, \tag{38}$$

B. Piezoelectric field in half-space GaAs

The polarization field is again related to the elastic strain tensor as in Eq. (19), and is found to be

$$P_x=2e_{14}\gamma_{yz}=-\frac{3\gamma^0 v_a e_{14}(1+\nu)y}{2\pi(1-\nu)}\left\{\frac{(z-h)}{R_1^5}+\frac{(z+h)}{R_2^5}\right.$$
$$\left.+\frac{2z}{R_2^5}-\frac{10z(z+h)^2}{R_2^7}\right\}. \tag{39}$$

While P_y can be obtained from P_x by replacing x with y, P_z has

$$P_z=2e_{14}\gamma_{xy}=-\frac{3\gamma^0 v_a e_{14}(1+\nu)xy}{2\pi(1-\nu)}\left\{\frac{1}{R_1^5}+\frac{3-4\nu}{R_2^5}\right.$$
$$\left.-\frac{10z(z+h)}{R_2^7}\right\}. \tag{40}$$

Using Eq. (21), we found the following Poisson's equation for the electric potential

$$\phi_{,kk}=\frac{\gamma^0 v_a e_{14}(1+\nu)xy}{2\pi(1-\nu)\epsilon_0\epsilon_r}\left\{\frac{45(z-h)}{R_1^7}+\frac{15(7-4\nu)(z+h)}{R_2^7}+\frac{90z}{R_2^7}-\frac{630z(z+h)^2}{R_2^9}\right\}. \tag{41}$$

Alternatively, this can be written as

$$\phi_{,kk}=\frac{\gamma^0 v_a e_{14}(1+\nu)}{2\pi(1-\nu)\epsilon_0\epsilon_r}\{-3(R_1^{-1})_{,xyz}+(5+4\nu)\times(R_2^{-1})_{,xyz}+6h(R_2^{-1})_{,xyzz}-6(R_2)_{,xyzzz}\}. \tag{42}$$

Since Eq. (42) needs to be solved with the given boundary condition on the surface of the half space, it is therefore convenient to express the electric potential as a sum of a particular and homogeneous solution, i.e.,

$$\phi=\phi^p+\phi^h, \tag{43}$$

where the first term on the right-hand side is a particular solution of Eq. (42) and the second term is the homogeneous solution added to satisfy the given piezoelectric boundary condition on the surface of the half space.

The particular solution of Eq. (42), after some simple but tedious derivations, is found to be

$$\phi^p=\frac{3\gamma^0 v_a e_{14}(1+\nu)xy}{4\pi(1-\nu)\epsilon_0\epsilon_r}\left\{\frac{-3(z-h)}{R_1^5}+\frac{(5+4\nu)(z+h)}{R_2^5}+6h\left[\frac{1}{R_2^5}-\frac{5(z+h)^2}{R_2^7}\right]-\frac{9(z+h)}{R_2^5}+\frac{15(z+h)^3}{R_2^7}\right\}. \tag{44}$$

For the homogeneous solution, which depends on the given boundary condition, the following two cases are discussed.

1. Traction-free conducting surface

For a conducting surface, we require that the electric potential on the surface $z=0$ vanishes, i.e., $\phi=0$. Using this condition along with Eqs. (43) and (44), the homogeneous solution for the electric potential is obtained as

$$\phi^h=\frac{3\gamma^0 v_a e_{14}(1+\nu)xy}{4\pi(1-\nu)\epsilon_0\epsilon_r}\left\{-\frac{(5+4\nu)h}{R_2^5}+\frac{15h^2(z+h)}{R_2^7}\right\}. \tag{45}$$

2. Traction-free insulating surface

Similarly, for an insulating surface, we require that $D_z=0$ on the surface $z=0$. For this case, the homogeneous solution for the electric potential can be expressed as

$$\phi^h(x,y,z)=\frac{3\gamma^0 v_a e_{14}(1+\nu)xy}{4\pi(1-\nu)\epsilon_0\epsilon_r}\left\{\frac{(1-4\nu)h}{R_2^5}+\frac{15h^2(z+h)}{R_2^7}\right\}+\frac{3\gamma^0 v_a e_{14}(1+\nu)(1-4\nu)}{8\pi^2(1-\nu)\epsilon_0\epsilon_r}\times\int_{-\infty}^{\infty}\int_{-\infty}^{\infty}\frac{k_x k_y}{[(k_x-x)^2+(k_y-y)^2+z^2]^{1/2}[k_x^2+k_y^2+h^2]^{5/2}}dk_x dk_y, \tag{46}$$

where the double Fourier integrals can be carried out using an efficient and adaptive quadrature proposed by Yang.[28]

With the electric potential being solved for both surface boundary conditions, the electric field can be found by taking the derivative of the electric potential. The electric displacement field is then obtained using Eq. (20c) along with the polarization fields (39) and (40).

VI. RESULTS

Having derived the elastic and piezoelectric solutions based on both the fully coupled and semicoupled models, we now carry out the comparison studies using these solutions. In the numerical study, we assume, for simplicity, that the mismatch eigenstrain in the QD is hydrostatic, i.e., $\gamma_{Ij}^*=\gamma^0\delta_{ij}$. We also assume that $\gamma^0=0.07$ for both the GaAs and AlN semiconductors,[24,25] although this eigenstrain is different for the latter case.[9] The QD is applied at the origin $\mathbf{x}=(0,0,0)$ for the full-space case (with no surface) and at $\mathbf{x}=(0,0,h)$ for the half-space case. For the examples presented next, the radius in the QD volume $v_a=4\pi a^3/3$ is fixed at $a=1$ nm, and the depth at $h=2$ nm (for the half-space case).

Material coefficients of the GaAs (001) are used for both the full and half spaces (i.e., for the half-space GaAs, the surface of the half space is in the [001] direction). The isotropic elastic constants (in 10^9 N/m^2) are $C_{11}=172$, $C_{12}=54$, and $C_{44}=59$ with a Poisson's ratio $\nu=0.2389$. We mention that while C_{12} and C_{44} are the elastic constants of GaAs,[2,29,30] C_{11} is obtained by the isotropic relation, i.e., $C_{11}=C_{12}+2C_{44}$. Also for GaAs, the only nonzero piezoelectric coefficient is e_{14} $(=e_{25}=e_{36})=-0.16$ C/m^2.[2,4] We remark that the negative sign in e_{14} was neglected in some previous publications based on the semicoupled model,[8,31,32] which gives the piezoelectric field with equal magnitude of, but opposite signs to, that using the right e_{14}. Finally, the relative dielectric constant is chosen as $\epsilon_r=12.5$.[8] Therefore, the electromechanical coupling factor g for GaAs, defined as $g=e_{\max}/\sqrt{(\epsilon_{\max}/C_{\max})}$, is found to be 0.04 (where $e_{\max}$, $\epsilon_{\max}$, and $C_{\max}$ are the maximum absolute values of the piezoelectric coefficients, dielectric constants, and elastic constants).

The elastic constants for AlN is (also in 10^9 N/m^2) $C_{11}=304$, $C_{12}=160$,[33] which gives $C_{44}=72$ by assuming isotropy. Therefore, the Poisson's ratio for this material is ν

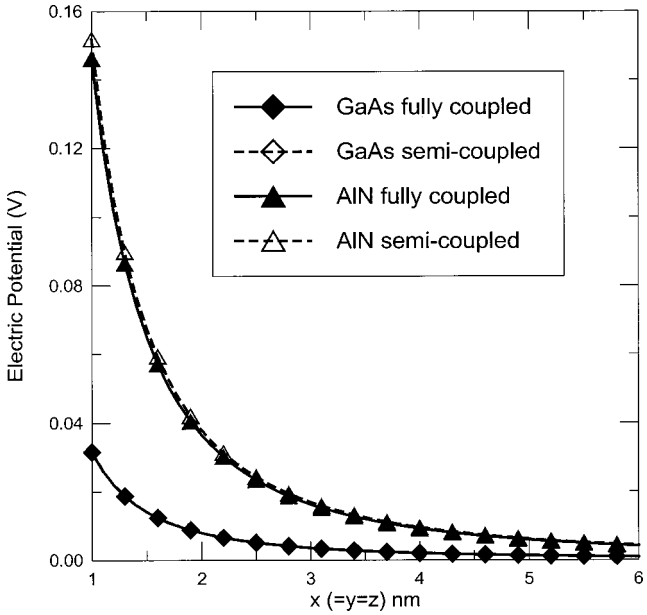

FIG. 2. Variations of the electric potential in GaAs and AlN along the line $\mathbf{x}=(x,x,x)$ due to a QD at the origin $\mathbf{x}=(0,0,0)$, predicted based on the fully coupled and semicoupled models.

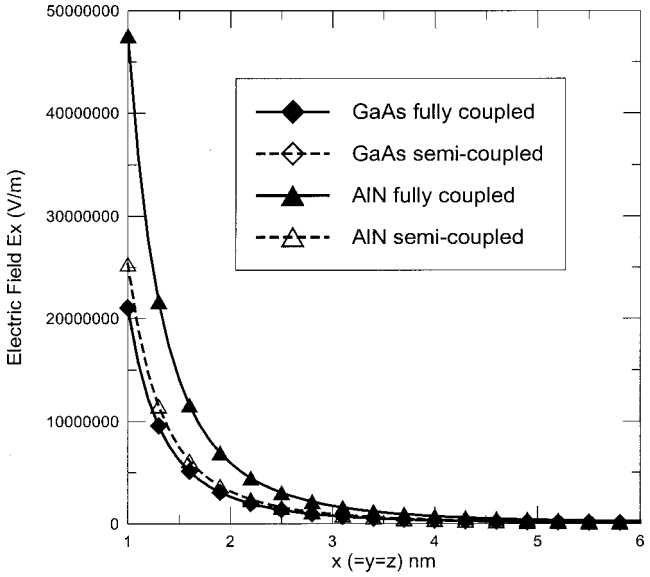

FIG. 3. Variations of the electric field E_x in GaAs and AlN along the line $\mathbf{x}=(x,x,x)$ due to a QD at the origin $\mathbf{x}=(0,0,0)$, predicted based on the fully coupled and semicoupled models.

$=0.3448$. The piezoelectric structure of AlN is transversely isotropic with poling direction along the z axis and has the following nonzero coefficients: $e_{33}=1.55$, $e_{31}(=e_{32})=-0.58$, and $e_{15}(=e_{24})=-0.48$ $(\mathrm{C/m^2})$.[9] Finally, the relative dielectric constant for AlN is $\epsilon_r=8.5$.[34] Similarly, the electromechanical coupling factor g for AlN is $g=0.32$, exactly eight times larger than that for GaAs.

A. Full-space GaAs and AlN

Shown in Fig. 2 are the variations of electric potential in the full-space GaAs and AlN along the line $\mathbf{x}=(x,x,x)$ due to the QD located at the origin $\mathbf{x}=(0,0,0)$, predicted based on the fully coupled and semicoupled models. We remark that while the electric potentials in GaAs and AlN along the line $\mathbf{x}=(x,x,0)$ and in GaAs along the line $\mathbf{x}=(0,0,z)$ are zero, the electric potential in AlN along the line $\mathbf{x}=(0,0,z)$ has a large magnitude (about ten times) as compared to that along the line $\mathbf{x}=(x,x,x)$. It is also observed from Fig. 2 that while both the fully coupled and semicoupled models predict nearly identical electric potential in GaAs, the electric potentials in AlN predicted based on the two models are different, in particular when the observation point is close to the QD.

Figure 3 shows the variation of the electric field E_x in GaAs and AlN along the line $\mathbf{x}=(x,x,x)$ due to the QD at the origin $\mathbf{x}=(0,0,0)$. Again, the electric fields in GaAs predicted based on both the fully coupled and semicoupled models are nearly the same. However, the electric fields in AlN based on the two models are substantially different, and in general, the semicoupled model underestimates the magnitude of the electric field. More specifically, at the observation point $\mathbf{x}=(x,x,x)=(1,1,1)$ nm, the magnitude of the electric field E_x predicted by the semicoupled model is roughly one half of that predicted based on the fully coupled model.

Since the piezoelectric field is directly related (or more specifically proportional) to the elastic field, one would expect that when using the semicoupled model to predict the elastic field, the result will be correct for GaAs and wrong for AlN. This is indeed the case. Similar to the electric quantities in GaAs, the elastic quantities in GaAs can also be very accurately predicted based on the semicoupled model. However, the elastic field in AlN can be wrong if the semicoupled model is used. For example, Fig. 4 shows the variations of the elastic strain field in AlN along the line $\mathbf{x}=(x,x,x)$ due to the QD at the origin $\mathbf{x}=(0,0,0)$, predicted based on both the fully coupled and semicoupled models. It is obvious that while the fully coupled model predicts nonzero strain com-

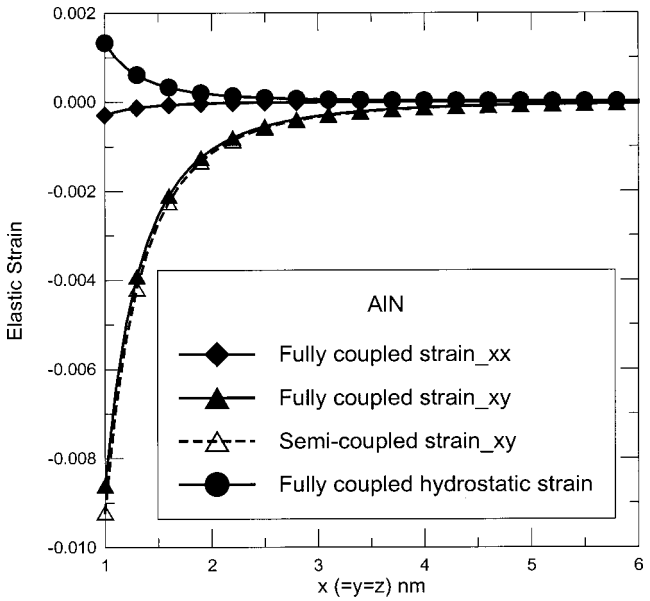

FIG. 4. Variations of the elastic strain in AlN along the line $\mathbf{x}=(x,x,x)$ due to a QD at the origin $\mathbf{x}=(0,0,0)$, predicted based on the fully coupled and semicoupled models.

ponent γ_{xx} and nonzero hydrostatic strain γ_{kk}, the semicoupled model gives zero results for them, as can be easily seen from Eqs. (23)–(25).

Our important observation on the elastic and piezoelectric fields induced by a QD in AlN has been further confirmed by applying the fully coupled and semicoupled models to a uniformly strained AlN layer grown along the polar axis.[35] Using the material properties for AlN,[9,36] we found that along the straining direction, the electric field predicted by the semicoupled model is 25% smaller than that based on the fully coupled model. More seriously, the predicted normal stresses in the straining direction based on the two models even have different signs (i.e., if the applied strain is of extension, the semicoupled and fully coupled models then predict a tensile and compressive stress, respectively).[35]

B. Half-space GaAs

By applying the semicoupled and fully coupled models to the full-space GaAs and AlN, we have been able to show that while the semicoupled model can predict accurate elastic and piezoelectric fields in semiconductor GaAs, it should not be used for AlN since otherwise substantial or serious errors may occur. An obvious reason is that GaAs is weakly coupled ($g=0.04$), while AlN is relatively strongly coupled ($g=0.32$).

In this section, we study the elastic and piezoelectric fields induced by a buried QD in a half-space GaAs, a case that has not been studied analytically in the literature. Assume that a QD is placed at $h=2$ nm below the surface of the half-space GaAs (Fig. 1), we have been able to show that for the two common types of surface conditions, i.e., traction-free conducting and traction-free insulating, the semicoupled model can still predict accurately the elastic and piezoelectric fields as compared to those based on the fully coupled model. Since such, we only present some piezoelectric results obtained using the fully coupled model and at the same time to show the influence of different surface conditions on the piezoelectric fields on the surface of the GaAs.

Depicted in Fig. 5 are the contours of the electric potential ϕ (10^{-2} V) on the traction-free and insulating surface of the half-space GaAs due to a QD of volume $v_a=4\pi a^3/3$ ($a=1$ nm) applied at $z=h$ ($=2$ nm). It is interesting that even though the present model uses a point QD the contour feature is still similar to that in Ref. 8. That is, the positive and negative electric potential values alternatively occupy one of the four quarters, with a maximum magnitude being 0.023 V.

While the contours of the horizontal electric field $E_h=\sqrt{E_x^2+E_y^2}$ (10^7 V/m) on the traction-free and insulating surface are shown in Fig. 6, those of the vertical electric field E_z (10^7 V/m) are presented in Fig. 7. It is observed that while the vertical electric field E_z follows the same feature as the electric potential with a maximum magnitude of 1.2×10^7 V/m, the horizontal electric field E_h shows an interesting feature. The horizontal electric field has a minimum at the center (the surface point directly above the QD), four equal maximums on both sides of the x and y axes, and four equal minimums on the diagonal axes $x=\pm y$. It should be also noticed that the maximum magnitude of the horizontal electric field can be as high as 3.5×10^7 V/m, the same magnitude as obtained in Ref. 1 for the corresponding superlattice case. We remark that these features have never been reported in the literature, and should be of interest to the design of strained QD semiconductor devices.

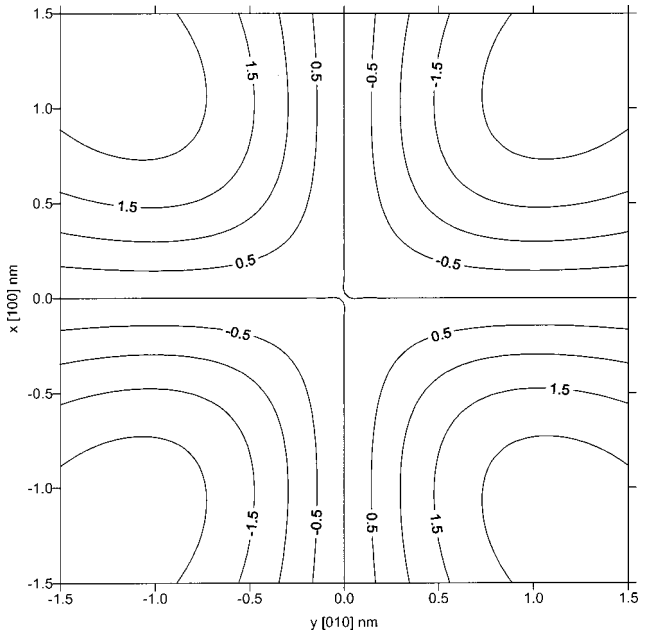

FIG. 5. Contours of the electric potential ϕ (10^{-2} V) on the traction-free and insulating surface of the half-space GaAs due to a QD at $h=2$ nm.

Finally, Fig. 8 shows the contours of the vertical electric field E_z (10^7 V/m) on the traction-free and conducting surface. The effect of different electric surface conditions on the vertical electric field can be observed by comparing Fig. 8

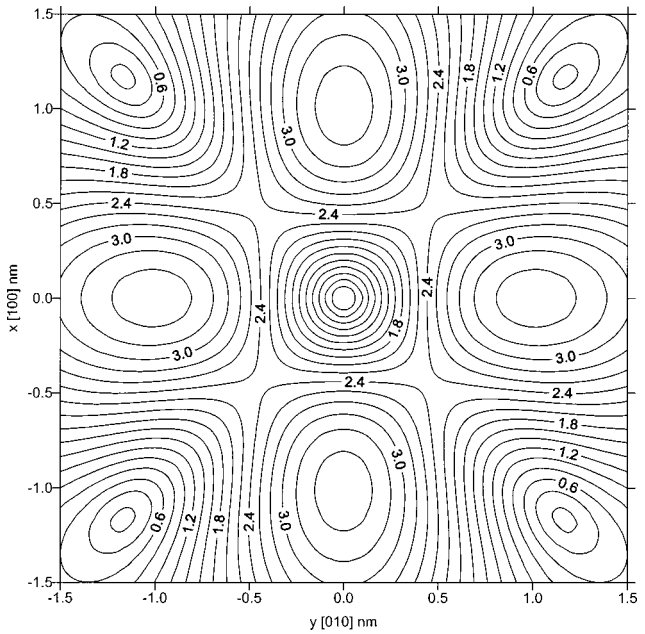

FIG. 6. Contours of the horizontal electric field $E_h=\sqrt{E_x^2+E_y^2}$ (10^7 V/m) on the traction-free and insulating surface of the half-space GaAs due to a QD at $h=2$ nm.

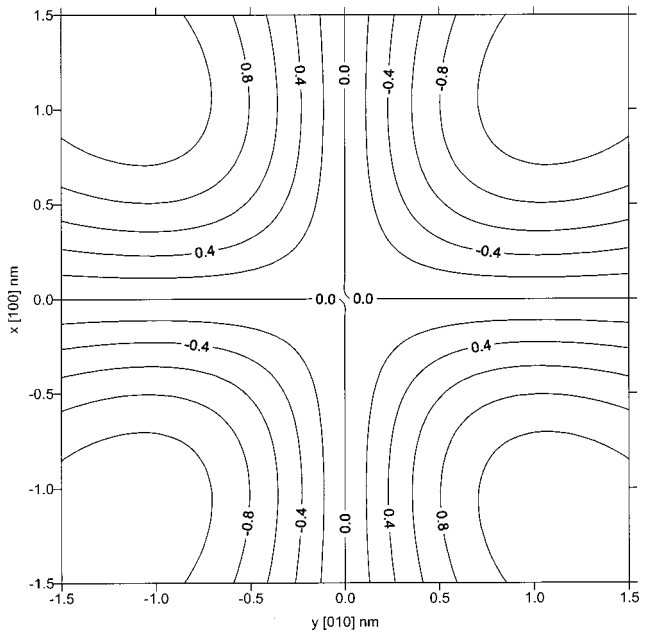

FIG. 7. Contours of the vertical electric field E_z (10^7 V/m) on the traction-free and insulating surface of the half-space GaAs due to a QD at $h=2$ nm.

with Fig. 7, and it is found that not only their magnitude, but also the locations of the maximum quantities are quite different. Specifically, much large magnitude for the vertical electric field E_z is observed if the surface is traction-free conducting, instead of traction-free insulating (2.7×10^7 vs 1.2×10^7 V/m). Therefore, by applying different piezoelectric conditions, one can not only relocate the position of maximum and/or minimum points of the piezoelectric field, but also change the magnitude of this field. This again should be of useful feature that can be applied to the design of semiconductor devices.

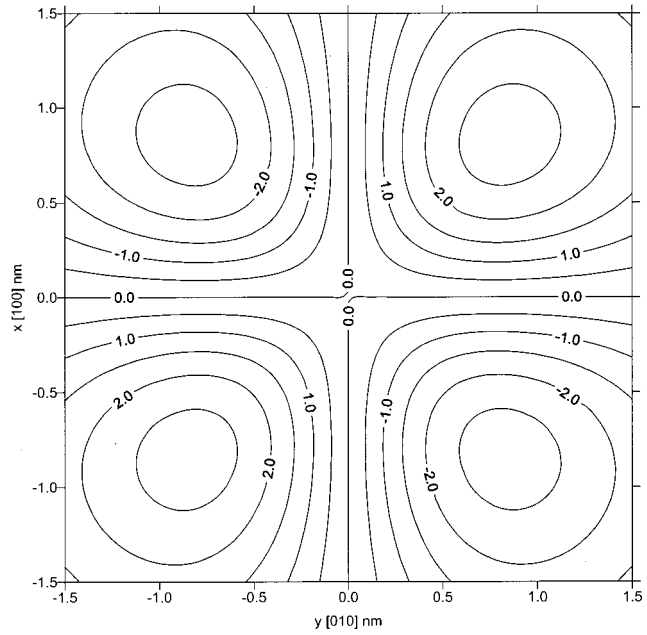

FIG. 8. Contours of the vertical electric field E_z (10^7 V/m) on the traction-free and conducting surface of the half-space GaAs due to a QD at $h=2$ nm.

VII. CONCLUSIONS

In this article, we have studied the elastic and piezoelectric fields in semiconductors GaAs and AlN due to a buried QD. By developing a fully coupled piezoelectric model and deriving the analytical solution for the semicoupled model, we have shown that the semicoupled piezoelectric model, adopted commonly in the physics community, is very accurate in the prediction of the elastic and piezoelectric fields in full- and half-space GaAs. However, use of the semicoupled model for AlN results in very serious errors for both the elastic and piezoelectric fields. Our observation on the elastic and piezoelectric fields in AlN has been further confirmed by applying the fully coupled and semicoupled models to a uniformly strained AlN layer grown along the polar axis. We remark that, in general, if a semiconductor possesses an electromechanical coupling factor $g\geqslant0.2$, then the fully coupled model should be used. The advantage of using the semicoupled model, instead of the fully coupled one, is apparent if an exact closed-form solution exists for the former. However, exact closed-form solution is available only when the elastic properties can be safely approximated as isotropic, which unfortunately may not be the case for most semiconductors, even for the GaAs.[2,24,25,29] Since isotropic and anisotropic semiconductors may response quite differently to the QD,[37] it is therefore suggested that the fully coupled piezoelectric model introduced in this article should be employed if a reliable result is required. The fully coupled piezoelectric model possesses the same structure as compared to the purely elastic and anisotropic model. Actually, one needs only to extend suitably the basic physical quantity dimension from 3 in elasticity (i.e., the three elastic displacement components) to 4 in piezoelectric (i.e., the three elastic displacement components plus the electric potential).

ACKNOWLEDGMENTS

The author would like to thank Professor C. Q. Ru and Dr. B. Yang for helpful discussions, and the reviewer for his constructive comments and suggestions. It is the reviewer who suggested the uniformly strained AlN layer model presented briefly in the article. This work, was partially supported by the AFOSR with Dr. Rick Hall as the program monitor.

APPENDIX A. FULL-SPACE GREEN'S FUNCTION

In this appendix, we briefly review the Green's functions in an anisotropic and linearly piezoelectric full space, while a detailed derivation can be found in Pan and Tonon.[18] These Green's functions include elastic displacement/electric potential, elastic stress/electric displacement, and their derivatives with respect to the source coordinates, due to a point force/point charge.

Assume that a point force/point charge is located at the origin of the space-fixed Cartesian coordinates (O, x_1, x_2, x_3), our purpose is then to find the complete three-dimensional Green's functions at the field point $\mathbf{x}$. We first

introduce an orthogonal and normalized system (O;**e**,**p**,**q**), with their base (**e**,**p**,**q**) being chosen as the following

$$\mathbf{e}=\mathbf{x}/r; \quad \mathbf{r}=|\mathbf{x}|. \tag{A1}$$

Now, let **v** be an arbitrary unit vector different from **e** (**v**≠**e**), the other two unit vectors orthogonal to **e** can then be selected as:

$$\mathbf{p}=\frac{\mathbf{e}\times\mathbf{v}}{|\mathbf{e}\times\mathbf{v}|}; \quad \mathbf{q}=\mathbf{e}\times\mathbf{p}. \tag{A2}$$

We define a matrix Γ_{jk} using the Stroh formalism[38] as

$$\Gamma(\mathbf{p}+\zeta\mathbf{q})\equiv\mathbf{Q}+\zeta(\mathbf{R}+\mathbf{R}^T)+\zeta^2\mathbf{T}, \tag{A3}$$

where

$$Q_{IK}=C_{jIKl}p_jq_l, \quad R_{IK}=C_{jIKl}p_jq_l, \quad T_{IK}=C_{jIKl}q_jq_l \tag{A4}$$

The determinant of $\Gamma(\mathbf{p}+\zeta\mathbf{q})$ is an eighth-order polynomial equation of ζ and has eight roots. In general, four of them are the conjugate of the remainder. These roots can be found either by expanding the determinant of $\Gamma(\mathbf{p}+\zeta\mathbf{q})$ into the polynomial, or by finding the eight eigenvalues of the following linear eigenequation[38]

$$\begin{bmatrix}\mathbf{N}_1 & \mathbf{N}_2\\ \mathbf{N}_3 & \mathbf{N}_1^T\end{bmatrix}\begin{bmatrix}\mathbf{a}\\ \mathbf{b}\end{bmatrix}=\zeta\begin{bmatrix}\mathbf{a}\\ \mathbf{b}\end{bmatrix}, \tag{A5}$$

where

$$\mathbf{N}_1=-\mathbf{T}^{-1}\mathbf{R}^T, \quad \mathbf{N}_2=\mathbf{T}^{-1}, \quad \mathbf{N}_3=\mathbf{R}\mathbf{T}^{-1}\mathbf{R}^T-\mathbf{Q} \tag{A6}$$

and **a** and **b** are the eigenvectors.

Assume that $\mathrm{Im}\,\zeta_M>0$ ($M=1,2,3,4$), and $\overline{\zeta}_M$ is the conjugate of ζ_M, the Green's tensor, with its first index for the elastic displacement/electric potential and the second index for the point force/point charge, can be finally expressed explicitly as

$$U_{IK}(\mathbf{x})=-\frac{\mathrm{Im}}{2\pi r}\sum_{M=1}^{4}\times\frac{A_{JK}(\mathbf{p}+\zeta_M\mathbf{q})}{a_9(\zeta_M-\overline{\zeta}_M)\prod_{\substack{L=1\\L\neq M}}^{4}(\zeta_M-\zeta_L)(\zeta_M-\overline{\zeta}_L)}, \tag{A7}$$

where $a_9=\det(\mathbf{T})$ is the coefficient of ζ^8, and A_{JK} are the co-factors of the matrix Γ_{JK}. It is now worthwhile to make some quick comments on the Green's function expression (A7): First, for a given pair of field and source points, one needs only to solve a eighth-order linear eigenequations (or a eighth-order polynomial equation) once in order to obtain all the components of the Green's tensor. Secondly, on obtaining Eq. (A7), we have assumed that all the poles are simple. Should the poles be multiple, a slight change in the material constants will result in single poles with negligible errors in the computed Green's tensor.[39,40] Thirdly, since Γ_{JK} is symmetric, so is its adjoint A_{JK}. Therefore, the Green's displacement G_{JK} is symmetric and one needs to calculate only 10 out of its 16 elements. Finally, although one can choose the vector **v** (≠**e**) arbitrarily, it should be one of the base vectors in the space-fixed Cartesian coordinates, i.e., (1,0,0), or (0,1,0), or (0,0,1). The analytical expression for the Green's displacement is much simpler using such a vector **v** than using any other vectors.

In the analysis of eigenstrain problems using the Green's function method, the first and second derivatives of the Green's tensor are also needed. These can be found using some simple yet accurate numerical formulations.[18,26]

APPENDIX B. HALF-SPACE GREEN'S FUNCTION

For the sake of easy reference, we also briefly present the Green's functions in an anisotropic and linearly piezoelectric half-space with traction-free insulating surface conditions. While a detailed derivation can be found in Pan and Yuan[19] for this special boundary condition, the reader is referred to Pan[10] for other general surface conditions. The piezoelectric half-space Green's function is expressed as a sum of the full-space Green's function presented in Appendix A and a complementary part, which resemble the Mindlin's solution for the corresponding elastic and isotropic half space.[41] The complementary part is expressed in terms of a regular line integral, which can be easily evaluated by a standard numerical quadrature.

We first introduce the extended Stroh eigenvalues and eigenvectors, which are mathematically elegant and numerically powerful.[38] These Stroh eigenvalue p_J and the corresponding 4×1 eigenvector $\mathbf{a}_J$ are the solutions of the following eigenrelation[19]

$$[\mathbf{Q}+p_J(\mathbf{R}+\mathbf{R}^T)+p_J^2\mathbf{T}]\mathbf{a}_J=0, \tag{B1}$$

where the superscript T denotes matrix transpose, and

$$Q_{IK}=C_{\alpha IK\beta}n_\alpha n_\beta, \quad R_{IK}=C_{\alpha IK3}n_\alpha, \quad T_{IK}=C_{3IK3} \tag{B2}$$

with

$$(n_1,n_2)\equiv(\cos\theta,\sin\theta) \tag{B3}$$

and α and β taking the values of 1 and 2. Similar to the full-space case, the eigenvalues of equation (B1) are either complex or purely imaginary due to the positive requirement on the strain energy density.

We then define other two vectors $\mathbf{b}_J$ (4×1) and $\mathbf{c}_J$ (5×1) related to the Stroh eigenvector $\mathbf{a}_J$ as

$$\mathbf{b}_J=(\mathbf{R}^T+p_J\mathbf{T})\mathbf{a}_J=-\frac{1}{p_J}(\mathbf{Q}+p_J\mathbf{R})\mathbf{a}_J, \tag{B4}$$

$$\mathbf{c}_J=\mathbf{D}_J\mathbf{a}_J,$$

where the 5×4 matrix $\mathbf{D}_J$ is defined by

$$(\mathbf{D}_J)_{kL}=\begin{cases}C_{1kL\alpha}n_\alpha+p_JC_{1kL3}(k=1,2)\\ C_{22L\alpha}n_\alpha+p_JC_{22L3}(k=3)\\ C_{i4L\alpha}n_\alpha+p_JC_{i4L3}(i=k-3)(k=4,5)\end{cases} \tag{B5}$$

Assume that p_J, $\mathbf{a}_J$, and $\mathbf{b}_J$ ($J=1,2,...,8$) are the distinct eigenvalues and the associated eigenvectors, we then choose

$$\begin{aligned}&\mathrm{Im}\, p_J>0, \quad p_{J=4}=\overline{p}_J, \quad \mathbf{a}_{J+4}=\overline{\mathbf{a}}_J, \quad \mathbf{b}_{J+4}=\overline{\mathbf{b}}_J,\\ &\mathbf{c}_{J+4}=\overline{\mathbf{c}}_J \quad (J=1,2,3,4)\\ &\mathbf{A}=[\mathbf{a}_1,\mathbf{a}_2,\mathbf{a}_3,\mathbf{a}_4], \quad \mathbf{B}=[\mathbf{b}_1,\mathbf{b}_2,\mathbf{b}_3,\mathbf{b}_4],\\ &\mathbf{C}=[\mathbf{c}_1,\mathbf{c}_2,\mathbf{c}_3,\mathbf{c}_4],\end{aligned} \tag{B6}$$

where Im stands for the imaginary part and the overbar denotes the complex conjugate, and the eigenvectors $\mathbf{a}_J$, and $\mathbf{b}_J$ satisfy

$$\mathbf{b}_I^T\mathbf{a}_J+\mathbf{a}_I^T\mathbf{b}_J=\delta_{IJ} \tag{B7}$$

with δ_{IJ} being the Kronecker delta.

Let us now denote by $\mathbf{U}^\infty(\mathbf{x};\mathbf{y})$ the full-space Green's function tensor given by (A7) of Appendix A with its row and column indices corresponding to the elastic displacement/electric potential and point force/point charge, respectively. Then, the half-space Green's tensor, with its components bearing the same physical meaning, can be written in a concise form as[10,19]

$$\mathbf{U}(\mathbf{x};\mathbf{y})=\mathbf{U}^\infty(\mathbf{x};\mathbf{y})+\frac{1}{2\pi^2}\int_0^\pi \overline{\mathbf{A}}\mathbf{G}_1\mathbf{A}^T d\theta, \tag{B8}$$

where

$$(\mathbf{G}_1)_{IJ}=\frac{(\overline{\mathbf{B}}^{-1}\mathbf{B})_{IJ}}{-\overline{p}_I x_3+p_J y_3-[(x_1-y_1)\cos\theta+(x_2-y_2)\sin\theta]}. \tag{B9}$$

Similarly, let $\mathbf{T}^\infty(\mathbf{x};\mathbf{y})$ and $\mathbf{S}^\infty(\mathbf{x};\mathbf{y})$ be the full-space Green's elastic stress/electric displacement with their components (or the row indices) being defined as

$$\begin{aligned}&(\mathbf{T}^\infty)|_{\mathrm{row}}=(\sigma_{31},\sigma_{32},\sigma_{33},D_3)^T,\\ &(\mathbf{S}^\infty)|_{\mathrm{row}}=(\sigma_{11},\sigma_{12},\sigma_{22},D_1,D_2)^T,\end{aligned} \tag{B10}$$

and their column indices for the point force/point charge. Then, the half-space Green's elastic stress/electric displacement can be derived as:[10,19]

$$\begin{aligned}&\mathbf{T}(\mathbf{x};\mathbf{y})=\mathbf{T}^\infty(\mathbf{x};\mathbf{y})+\frac{1}{2\pi^2}\int_0^\pi \overline{\mathbf{B}}\mathbf{G}_2\mathbf{A}^T d\theta,\\ &\mathbf{S}(\mathbf{x};\mathbf{y})=\mathbf{S}^\infty(\mathbf{x};\mathbf{y})+\frac{1}{2\pi^2}\int_0^\pi \overline{\mathbf{C}}\mathbf{G}_2\mathbf{A}^T d\theta.\end{aligned} \tag{B11}$$

In Eqs. (B11),

$$(\mathbf{G}_2)_{IJ}=\frac{(\overline{\mathbf{B}}^{-1}\mathbf{B})_{IJ}}{\{-\overline{p}_I x_3+p_J y_3-[(x_1-y_1)\cos\theta+(x_2-y_2)\sin\theta]\}^2}. \tag{B12}$$

Derivatives of the Green's elastic displacement/electric potential with respect to the source point (y_1,y_2,y_3) can be easily carried out and the results are:

$$\frac{\partial\mathbf{U}(\mathbf{x};\mathbf{y})}{\partial y_j}=\frac{\partial\mathbf{U}^\infty(\mathbf{x};\mathbf{y})}{\partial y_j}-\frac{1}{2\pi^2}\int_0^\pi \overline{\mathbf{A}}\mathbf{G}_2\langle g_j\rangle\mathbf{A}^T d\theta, \tag{B13}$$

where

$$\begin{aligned}&\langle g_1\rangle=\mathrm{diag}[\cos\theta,\cos\theta,\cos\theta,\cos\theta],\\ &\langle g_2\rangle=\mathrm{diag}[\sin\theta,\sin\theta,\sin\theta,\sin\theta],\\ &\langle g_3\rangle=\mathrm{diag}[p_1,p_2,p_3,p_4].\end{aligned} \tag{B14}$$

Similarly, the derivatives of the Green's elastic stress/electric displacement with respect to the source point (y_1,y_2,y_3) are:

$$\begin{aligned}&\frac{\partial\mathbf{T}(\mathbf{x};\mathbf{y})}{\partial y_j}=\frac{\partial\mathbf{T}^\infty(\mathbf{x};\mathbf{y})}{\partial y_j}-\frac{1}{2\pi^2}\int_0^\pi \overline{\mathbf{B}}\mathbf{G}_3\langle g_j\rangle\mathbf{A}^T d\theta,\\ &\frac{\partial\mathbf{S}(\mathbf{x};\mathbf{y})}{\partial y_j}=\frac{\partial\mathbf{S}^\infty(\mathbf{x};\mathbf{y})}{\partial y_j}-\frac{1}{2\pi^2}\int_0^\pi \overline{\mathbf{C}}\mathbf{G}_3\langle g_j\rangle\mathbf{A}^T d\theta,\end{aligned} \tag{B15}$$

where

$$(\mathbf{G}_3)_{IJ}=\frac{(\overline{\mathbf{B}}^{-1}\mathbf{B})_{IJ}}{\{-\overline{p}_I x_3+p_J y_3-[(x_1-y_1)\cos\theta+(x_2-y_2)\sin\theta]\}^3} \tag{B16}$$

Equations (B8), (B11), (B13), and (B15) are the complete Green's functions in an anisotropic and linearly piezoelectric half space with traction-free insulating boundary conditions, or the generalized Mindlin solution in anisotropic piezoelectric half space. Mindlin solutions to other types of surface boundary conditions, along with some typical numerical examples can be found in Pan.[10]

[1] D. L. Smith, Solid State Commun. **57**, 919 (1986); D. L. Smith and C. Mailhiot, Rev. Mod. Phys. **62**, 173 (1990).
[2] S. Adachi, J. Appl. Phys. **58**, R1 (1985).
[3] D. Bimberg, M. Grundmann, and N. N. Ledentsov, *Quantum Dot Heterostructures* (Wiley, New York, 1998).
[4] J. H. Davies, J. Appl. Phys. **84**, 1358 (1998); J. H. Davies, Appl. Phys. Lett. **75**, 4142 (1999); J. H. Davies and I. A. Larkin, Phys. Rev. B **49**, 4800 (1994).
[5] C. Pryor, M. E. Pistol, and L. Samuelson, Phys. Rev. B **56**, 10404 (1997); C. Pryor *et al.*, Appl. Phys. Lett. **83**, 2548 (1998); X. Z. Liao *et al.*, Phys. Rev. Lett. **82**, 5148 (1999).
[6] T. Benabbas, P. Francois, Y. Androussi, and A. Lefebvre, J. Appl. Phys. **80**, 2763 (1996).
[7] S. Kret *et al.*, J. Appl. Phys. **86**, 1988 (1999).
[8] M. Grundmann, O. Stier, and D. Bimberg, Phys. Rev. B **52**, 11969 (1995).
[9] A. D. Bykhovski, R. Gaska, and M. S. Shur, Appl. Phys. Lett. **73**, 3577 (1998); B. Jogai, J. Appl. Phys. **90**, 699 (2001).
[10] E. Pan, Proc. R. Soc. London, Ser. A **458**, 181 (2002).
[11] C. Q. Ru, Proc. R. Soc. London, Ser. A **456**, 1051 (2000).
[12] C. Q. Ru, Proc. R. Soc. London, Ser. A **468**, 265 (2001).
[13] E. Pan, Eng. Anal. Bound. Elements **23**, 67 (1999).
[14] H. F. Tiersten, Linear Piezoelectric Plate Vibrations (Plenum, New York, 1969).
[15] D. M. Barnett and J. Lothe, Phys. Norv. **8**, 13 (1975).
[16] J. F. Nye, *Physical Properties of Crystals* (Clarendon, Oxford, 1985).
[17] M. L. Dunn and M. Taya, Proc. R. Soc. London, Ser. A **443**, 265 (1993).
[18] E. Pan and F. Tonon, Int. J. Solids Struct. **37**, 943 (2000).
[19] E. Pan and F. G. Yuan, Int. J. Eng. Sci. **38**, 1939 (2000).
[20] E. Pan, Acta Mech. **87**, 105 (1991).
[21] A. H. D. Cheng and E. Detournay, Int. J. Solids Struct. **35**, 4521 (1998).
[22] T. Mura, *Micromechanics of Defects in Solids* 2nd. ed. (Kluwer, Dordrecht, 1987).
[23] H. Y. Yu and S. C. Sanday, Proc. R. Soc. London, Ser. A **434**, 503 (1991).
[24] D. A. Faux and G. S. Pearson, Phys. Rev. B **62**, R4798 (2000).
[25] G. S. Pearson and D. A. Faux, J. Appl. Phys. **88**, 730 (2000).
[26] E. Tonon, E. Pan, and B. Amadei, Comput. Struct. **79**, 469 (2001).

[27] R. D. Mindlin and D. H. Cheng, J. Appl. Phys. **21**, 926 (1950).
[28] B. Yang (unpublished).
[29] M. P. C. M. Krijn, Semicond. Sci. Technol. **6**, 27 (1991).
[30] A. D. Andreev, J. R. Downes, D. A. Faux, and E. P. O'Reilly, J. Appl. Phys. **86**, 297 (1999).
[31] O. Stier, M. Grundmann, and D. Bimberg, Phys. Rev. B **59**, 5688 (1999).
[32] B. W. Kim, J. Appl. Phys. **89**, 1197 (2001).
[33] A. F. Wright, J. Appl. Phys. **82**, 2833 (1997).
[34] V. W. L. Chin, T. L. Tansley, and T. Osotchan, J. Appl. Phys. **75**, 7365 (1994).
[35] E. Pan and B. Yang (unpublished).
[36] J. G. Gualtieri, J. A. Kosinski, and A. Ballato, IEEE Trans. Ultrason. Ferroelectr. Freq. Control **41**, 53 (1994).
[37] E. Pan and B. Yang, J. Appl. Phys. **90**, 6190 (2001).
[38] T. C. T. Ting, *Anisotropic Elasticity* (Oxford University Press, Oxford, 1996).
[39] E. Pan and B. Amadei, Int. J. Fract. **77**, 161 (1996).
[40] E. Pan, Int. J. Fract. **88**, 41 (1997).
[41] R. D. Mindlin, Physics (N.Y.) **7**, 195 (1936).